Silke Hügl*, Tobias Blum, Thomas Lenarz, Omid Majdani, and Thomas S. Rau

Impact of anatomical variations on insertion forces

An investigation using artificial cochlear models

Abstract: The choice of a cochlear implant electrode carrier for the individual patient is influenced by cochlear size, as this parameter has an impact on the risk of scala dislocations. Therefore, size and morphology should be represented in artificial cochlear models too, since these are generally used for insertion studies evaluating newly developed cochlear implant electrode carriers and insertion techniques, before human temporal bone studies are applied for. Within this study custom-made electrode carrier test samples were inserted into nine artificial cochlear models of different shape. To fabricate them, four human temporal bone samples have been processed by a serial cross-sectioning technique; the other four samples have been scanned with micro computed tomography. The cochlea was segmented on this data using rotating, midmodiolar slice planes, followed by the generation of a three-dimensional digital model, which finally was projected on a plane and 2D models were milled out of PTFE. The ratios of length to width of the cochlear basal turn of our samples were found to be within previously reported range. For comparative reasons a model used in previous studies was included in this study too. The maximal insertion forces per cochlear model followed a normal distribution. The insertion depth at initial insertion force increase is correlated to the length of cochlear basal turn. Using the here presented cochlear models with varying anatomical measures may help to increase the clinical relevance of insertion studies in artificial cochlear models.

Keywords: cochlear size, A- and B-value, insertion force

https://doi.org/10.1515/cdbme-2018-0122

***Corresponding author: Silke Hügl:** Hannover Medical School, Department of Otolaryngology, Carl-Neuberg-Strasse 1, 30625 Hannover, Germany, huegl.silke@mh-hannover.de
Tobias Blum, Thomas Lenarz, Omid Majdani, Thomas S. Rau: Department of Otolaryngology and Cluster of Excellence EXC 1077/1 “Hearing4all”, Hannover Medical School, Hannover, Germany

1 Motivation

The cochlear implant is a neuroprosthesis for the treatment of severe to profound hearing loss. The electrode carrier of the cochlear implant is inserted into the spiral shaped organ of the cochlea during surgery, to apply electrical stimuli directly to neurons. Any malfunctioning hair cells inside the cochlea, which normally transform sound in the form of fluid movement within the cochlea into electrical stimuli, are bypassed.

In biomedical research insertion studies of cochlear implant electrode carriers into human temporal bone samples (which include the cochlea) or artificial cochlear models are widely used for experimental validation of newly developed electrode carriers [1], changed insertion protocols due to use of coatings or lubricants [2] or for the validation of adapted surgical approaches [3].

Such insertion studies are analysed using insertion force measurements and, in case of human temporal bone samples, histological evaluations. In these cases low insertion forces and the lack of intra-cochlear trauma are regarded beneficial. Experiments with human temporal bone samples show the most relevant conditions for evaluating the effect of anatomical variation on the insertion process and forces. Unfortunately, the comparability of such studies is limited, as the mechanical characteristics of tissue within the cochlea may vary due to duration and condition (cooled, frozen, fixed) of storage until starting the experiments [4]. Additionally, repeated insertions into one temporal bone sample may be problematic, as potential intra-cochlear trauma of earlier insertion may change the intra-cochlear structures with an impact on subsequent insertions [5]. Therefore stable conditions for repeated experiments into one temporal bone sample cannot be assured.

The aim of the presented study was to provide anatomical relevant variation with otherwise identical artificial cochlear models and show that characteristics of the insertion force profile depend on the specific geometry. Thus, repeatable experiments under stable conditions into a variety of artificial cochlear models, whose geometrical measures are based on individual human samples, are enabled.

2 Material and methods

2.1 Cochlear implant test samples

The custom-made test samples have a length of 17.2 mm with a decreasing diameter from base to tip (0.8 mm to 0.5 mm), completed with a tapered tip (diameter 0.2 mm). In order to mimic the cable bundle within, four copper wires (diameter: 0.07 mm) with graded lengths were embedded into the blue dyed silicone (Sylgard 184, Dow, Midland USA) test samples. For fabrication, a two-piece casting mould was filled with the copper wires and the silicone and finally cured at 60 °C for 2.5 hours.

2.2 Fabrication of cochlear models

Nine planar artificial cochlear models made of polytetrafluoroethylene (PTFE), each filled with soap solution (10% soap, 90% water) and covered with an acrylic glass disk, have been used. The geometry for the first model was previously described [6].

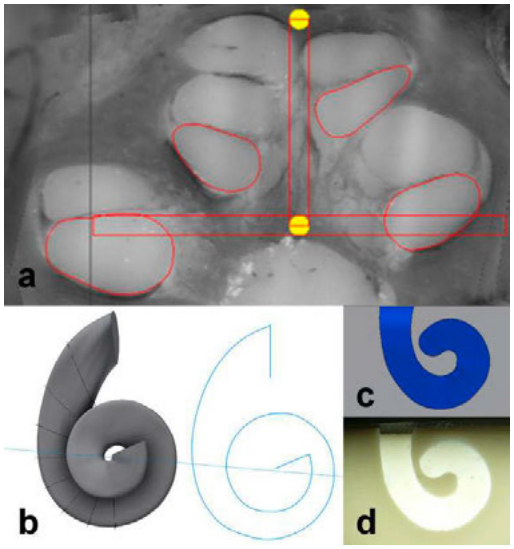

Figure 1: Generation of the cochlear models through scala tympani segmentation (a), with the modiolar axis as line between the yellow dots. Following the 3D-modell is generated, projected onto a plane (b) and finally the geometry is transferred to a planar model (c) fabricated out of PTFE (d).

The other eight models are fabricated based on individual geometry of segmented human temporal bone samples, chosen out of a large variety of samples. Four human temporal bone samples were scanned using micro computed tomography (µCT100, Scanco Medical AG, Brüttisellen, Switzerland) to receive DICOM data. Four additional human temporal bone samples were processed with a serial cross-sectional morphological imaging technique (microgrinding:[7-8]). These eight samples have been gathered within a previous study.

The datasets were chosen for a preferably large range of A- and B-values and visualized in midmodiolar slice planes, rotating around the modiolar axis of the spiral shaped cochlea using a custom DICOM viewer [9]. Within these slices, every 22.5 ° beginning at the round window, the scala tympani was segmented (see Fig 1). Post-processing led to a three-dimensional (3D) model within CAD software (Autodesk Inventor, Autodesk Co., USA).

The outer contour of each 3D scala tympani volume was projected onto a plane to derive the planar geometry. For better comparability the geometry was mirrored if needed to derive a counter-clockwise rotation of the scala tympani lumen. Each artificial PTFE cochlear model was fabricated using a computer numerically controlled (CNC) mill. An acrylic glass disk to cover the model was provided for visual documentation of the insertion.

2.3 Insertion and force measurement

Insertions were conducted by a linear translation stage (LTM-80M-270, Owis GmbH, Staufen, Germany) using an insertion speed of 0.4 mm/s. Test samples were gripped with surgical forceps (KARL STORZ GmbH & Co. KG, Tuttlingen, Germany) mounted on the translation stage. Cochlear models were filled with soap solution and mounted on a 3D-force sensor (K3D35, ME-Meßsysteme GmbH, Hennigsdorf, Germany) with 0.5 N nominal force. A custom-made software tool controlled insertion and force measurement. Force sensor output was verified using check weights before insertion. A test insertion with an additional test sample, only used for this purpose, was conducted to verify the orientation of the insertion axis after each exchange of the cochlear model. One test sample was inserted once into all nine cochlear models. The following eight test samples each rotated the cochlear model at the start of insertion order (see Tab. 1). This protocol was followed twice, leading to a total of 162 insertions with 18 test samples.

Table 1: Insertion order for nine test samples. This procedure was followed twice, leading to a total of 18 used test samples.

		Cochlear Models								
		old	newly derived cochlear models							
		1	2	3	4	5	6	7	8	9
A-value (mm)		10.4	8.3	8.9	9.2	9.3	9.3	9.7	9.8	9.8
B-value (mm)		6.1	6.0	7.2	6.6	6.4	6.7	6.7	7.4	7.5
Test samples	1 / 10	1	2	3	4	5	6	7	8	9
	2 / 11	9	1	2	3	4	5	6	7	8
	3 / 12	8	9	1	2	3	4	5	6	7
	4 / 13	7	8	9	1	2	3	4	5	6
	5 / 14	6	7	8	9	1	2	3	4	5
	6 / 15	5	6	7	8	9	1	2	3	4
	7 / 16	4	5	6	7	8	9	1	2	3
	8 / 17	3	4	5	6	7	8	9	1	2
	9 / 18	2	3	4	5	6	7	8	9	1

3 Results

Five test samples, out of 18 which were used in total, had to be removed from analysis due to considerable buckling during insertion (four samples) and because of a copper wire sticking out of the silicone body (one sample). This led to 13 evaluated insertions per cochlear model (see Fig. 2).

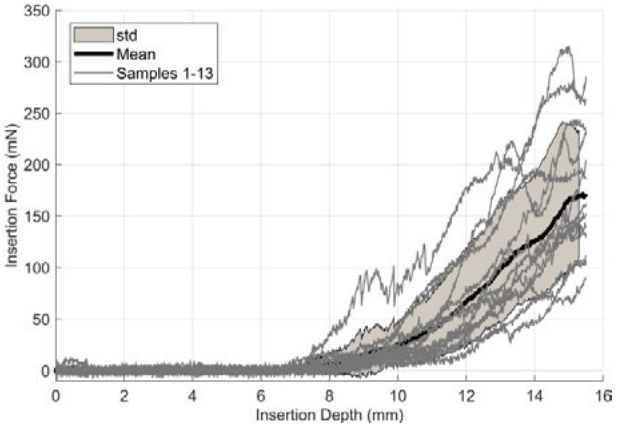

Figure 2: Insertions into one cochlear model with mean forces and standard deviation (exemplarily shown for model one).

Maximal insertion forces occurred at the end of insertion and have been averaged for each model (see Fig. 1-3). The maximal forces at the end of insertion follow a normal distribution (Shapiro-Wilk-test) for all cochlear models, although models 8 and 9 each show one high outlier, which was therefore neglected for this testing. The insertion profiles show statistically significant differences (Wilcoxon, $p < 0.05$), except for models 1 and 8.

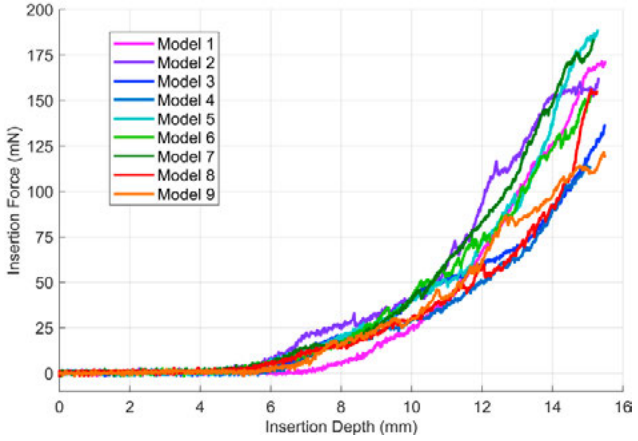

Figure 3: Mean Insertion forces for all nine cochlear models

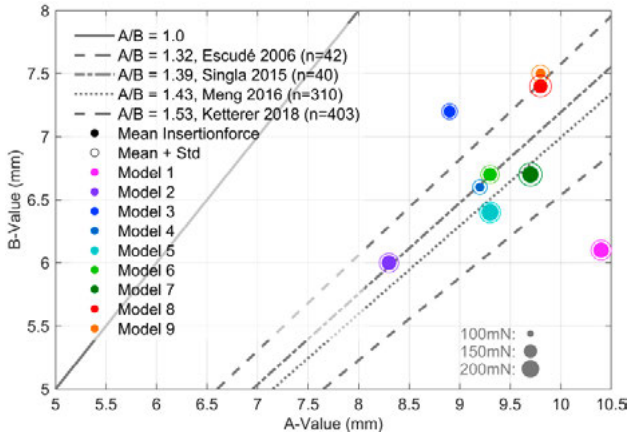

Figure 4: Length and width (A-/B-value) of cochlear basal turn. With an A/B-ratio of 1, basal turn would be circular. A/B-ratio from literature [10-13] shown as comparison. Maximal insertions forces at the end of insertion procedure are shown as size of the circles.

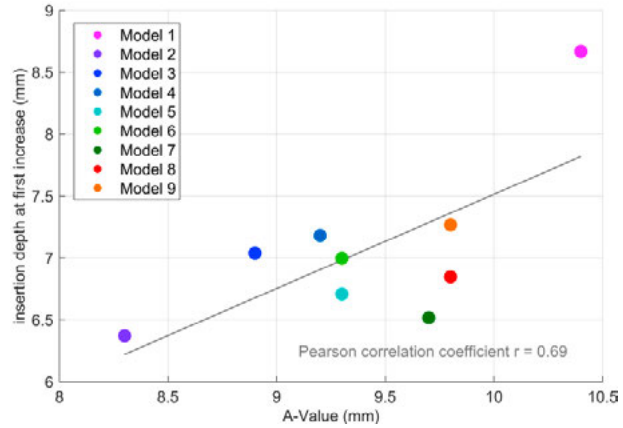

Figure 5: Cochlea basal turn length (A-value) correlates with the insertion depth of initial force increase (threshold 10mN).

The insertion depth at which the mean curves of each model finally rose above 10mN was evaluated. This depth was found to be significantly correlated (Pearson $r = 0.69$, $p < 0.05$) to the length of the cochlear basal turn (A-value). The shorter the A-value is, the earlier the insertion force increases (see Fig.4). The width of the cochlear basal turn (B-value) was found to be correlated to the maximal insertion force (Pearson $r = -0.51$, no significance).

4 Discussion

The presented study evaluated insertions into 9 differently sized artificial cochlear models. Characteristic insertion profiles vary significantly for eight models. A- and B-value show correlations to the observable force profiles, although the shown results should be interpreted as tendency since the variance in insertion forces was higher than with insertions using commercial electrode carriers.

An important step in the development of new electrode carriers or assistance systems as insertion tools is intensive testing under clinically relevant conditions. That applies especially to geometry, material properties and fluid filling of the insertion models. To avoid overfitting of new developments to one specific model, a number of morphologically different cochlear models is needed. Furthermore cochlear size and morphology is one of the parameters used clinically to decide what electrode array to choose for the individual patient. Ketterer et al. (2018) investigated 403 implanted ears and found more scala dislocations for smaller cochlear widths (B-value) [13]. These observations place the necessity for cochlear models representing anatomical variation, which enable repeated and reproducible experiments.

Author Statement

Research funding: German Research Foundation (DFG), Cluster of Excellence EXC 1077/1 “Hearing4all”. Conflict of interest: Authors state no conflict of interest. Informed consent: Informed consent is not applicable. Ethical approval: The conducted research is not related to either human or animals use.

References

[1] Majdani O, Lenarz T, Pawsey N, Risi F, Sedlmayr G, Rau TS. First results with a prototype of a new cochlear implant electrode featuring shape memors effect. Biomed Eng-Biomed Tech 2013;58 (Suppl 1).

[2] Kontorinis G, Paasche G, Lenarz T, Stöver T. The effect of different lubricants on cochlear implant electrode insertion forces. Otology & Neurotology 2011; 32:1050–1056.

[3] Majdani O, Schurzig D, Hussong A, Rau TS, Wittkopf J, Lenarz T, et al. Force measurement of insertion of cochlear implant electrode arrays in vitro: comparison of surgeon to automated insertion tool. Acta oto-laryngologica 2010: 130:31–36.

[4] De Seta D, Torres R, Russo FY, Ferrary E, Kazmitcheff G, Heymann D, et al. Damage to inner ear structure during cochlear implantation: Correlation between insertion force and radio-histological findings in temporal bone specimens. Hearing research 2016; 344:90–97.

[5] Roland JT. A model for cochlear implant electrode insertion and force evaluation: results with a new electrode design and insertion technique. The Laryngoscope 2005; 115:1325–1339.

[6] Todd CA, Naghdy F, Svehla MJ. Force application during cochlear implant insertion: an analysis for improvement of surgeon technique. IEEE transactions on biomedical engineering 2007; 54:1247-1255.

[7] Rau TS, Würfel W, Lenarz T, Majdani O. Three-dimensional histological specimen preparation for accurate imaging and spatial reconstruction of the middle and inner ear. International journal of computer assisted radiology and surgery 2013; 8:481-509.

[8] Hügl S, Eckardt F, Lexow GJ, Majdani O, Lenarz T, Rau TS. Increasing the resolution of morphological 3D image data sets through image stitching: application to the temporal bone. Computer Methods in Biomechanics and Biomedical Engineering: Imaging & Visualization, 2017; 5:438-445.

[9] Lexow GJ, Schurzig D, Gellrich NC, Lenarz T, Majdani O, Rau TS. Visualization, measurement and modelling of the cochlea using rotating midmodiolar slice planes. International journal of computer assisted radiology and surgery 2016; 11:1855-1869.

[10] Escudé B, James C, Deguine O, Cochard N, Eter E, Fraysse B. The size of the cochlea and predictions of insertion depth angles for cochlear implant electrodes. Audiology and Neurotology 2006; 11:27-33.

[11] Singla A, Sahni D, Gupta AK, Aggarwal A, Gupta T. Surgical anatomy of the basal turn of the human cochlea as pertaining to cochlear implantation. Otology & Neurotology 2015; 36:323-328.

[12] Meng J, Li S, Zhang F, Li Q, Qin Z. Cochlear size and shape variability and implications in cochlear implantation surgery. Otology & Neurotology 2016; 37:1307-1313.

[13] Ketterer MC, Aschendorff A, Arndt S, Hassepass F, Wesarg T, Laszig R, et al. The influence of cochlear morphology on the final electrode array position. European Archives of Oto-Rhino-Laryngology 2018; 275:385-394.